

Simulation of Agricultural Soil Tillage Machine using DEM

Hagop Mouradjalian¹, Zvika Asaf¹, Itzhak Shmulevich¹, Boaz Zion²,

¹Agricultural engineering research center, Civil and Environmental engineering – Technion Israel Institute of Technology, Haifa, Israel.

²Israeli Agricultural Research Organization – Volcani Center, Beit Dagan, Israel.

Abstract

The Israeli Agricultural Research Organization – Volcani Center developed a machine for weed (Nutsedge) pest control. In front of the machine a large blade is placed which penetrates into the soil, tills and directs the soil onto the conveyor.

The aim of this work is to simulate the machine-soil interaction as a tool for better machine design and to reduce the power requirements of the machine by the developed tool. The reported work used LS-DYNA dynamic analysis for modeling the machine by Lagrangian elements and the soil by cohesive Discrete Element (DE) particles to represent clayey soil. The parametric examination using the developed model showed significant difference in the drag forces between different blade designs and different blade orientations.

The simulation was calibrated and validated by full scale experiments using the soil tillage machine pulled by a tractor at an agricultural field. During the experiments several parameters were measured: the soil stiffness in field, the drag forces and their direction, the tillage velocity and the depth of tillage. The experimental work validated the simulation. The results of the research show that over 30% power reduction can be obtained by improved design of the blade's shape, angle and position.

1 Introduction

Agricultural soil tillage machines for root crops harvesting such as potato and onion as well as other soil tillage machines penetrate into the ground during operation and convey large amount of soil or root crops over a tilted pickup chain conveyor. These types of machines sustain extremely large loads that require heavy pulling tractors. The Israeli Agricultural Research Organization – Volcani Center developed such a machine for weed (Nutsedge) pest control. Fig. 1 shows images of the developed machine. In this machine as in many others a large blade is placed in front of the conveyor which penetrates into the soil, tills the soil at a required operation depth and directs the tilled soil onto a pickup chain conveyor.



Fig. 1: Nutsedge pest control tillage machine.

The operating method of this machine is by tilling the soil at an arbitrary operation depth and elevating the soil onto its vibrating chain conveyors. Small soil particles drop through the gaps of the conveyors, afterwards large soil aggregates fall behind the machine on top of the surface. The nuts of the Nutsedge weed are mainly connected to the large soil aggregates as shown in Fig. 2. Exposure of large soil aggregates along with the nuts to the sun for several weeks period causes the nuts to dry and prevents further Nutsedge growth.



Fig.2: Nutsedge weed and its nut connected to a large soil aggregate.

The mechanical design of the tillage blade and its position relative to the pickup conveyor has a great impact on the power efficiency of the machine. A small change in the operating angle of the blade or its position relative to the pickup conveyor can have a significant impact on the operation of the machine and on the acting drag forces that in turn might cause a significant waste of energy. Simulation of the agricultural soil tillage machine is important for power consumption reduction during tillage processes.

The agricultural engineering research center at the Technion has many years of modeling experience using the Discrete Element Method (DEM). Asaf et. al. [1-3] and Shmulevich et. al. [4-5] used the DE method for machine-soil interaction modeling. Shmulevich et. al. [6] demonstrated the use of DE method for cohesive grain materials modeling with experimental verification. The aim of this research is to simulate the machine-soil interaction as a tool for better machine design and to reduce the power requirements of the machine by the developed tool. The reported work used LS-DYNA dynamic analysis for modeling the machine by Lagrangian elements and the soil by cohesive Discrete Element (DE) particles to represent clay soil. Optimization of the blade's shape, the position of the conveyor and their combination by trial and error experiments would be a long and expensive process.

2 Full scale field experiment

A full scale experiment was conducted at a plowed agricultural clayey field in order to calibrate and verify the simulation model. During the experiment the tillage machine was pulled by a John Deere tractor 6190R as shown in Fig. 3. Two adjustable front wheels were added to the machine in order to keep the depth of the tillage constant. Six field runs were conducted with the following parameters: 2 velocities (1.2 and 1.8 km/h), 2 blades with different length and angle (52.5 cm @ 19° and 37.5 cm @ 27.5°) and 2 operation depths (30 cm and 35 cm). At a depth of 35 cm only two trials were made because the tractor could not pull the developed high loads.



Fig.3: Full scale tillage machine field drag experiment.

The tillage machine was equipped with sensors and a data acquisition system controlled and real time monitored by an operator with laptop at the tractor's cabin. During the experiments several parameters were measured: the drag forces and their direction, the tillage velocity and the depth of tillage. The acquisition system and the sensors are presented in Fig. 4. The tillage machine was connected to the bottom two arms of the tractor's three point arm system with two force transducers. A tilt sensor was mounted on the force transducer to determine the force components. A laser distance sensor was mounted on the front part of the frame in order to measure the tillage depth. On the rear wheel an encoder was attached with a pendulum arm and a spring in order to measure the tillage velocity.



Fig.4: Acquisition system and sensors at the experiment.

Two types of tests were conducted in order to estimate the inhomogeneity of the soil with depth: laboratory water content measurement and in situ soil stiffness evaluation with a dynamic cone penetrometer. The soil water content results and the dynamic cone penetrometer test setup are presented in Fig. 5. The water content values increased with depth ranging from 4% to 15% at soil surface and to depth of 50 cm respectively. The results of the dynamic cone penetrometer test are presented in chapter 4.

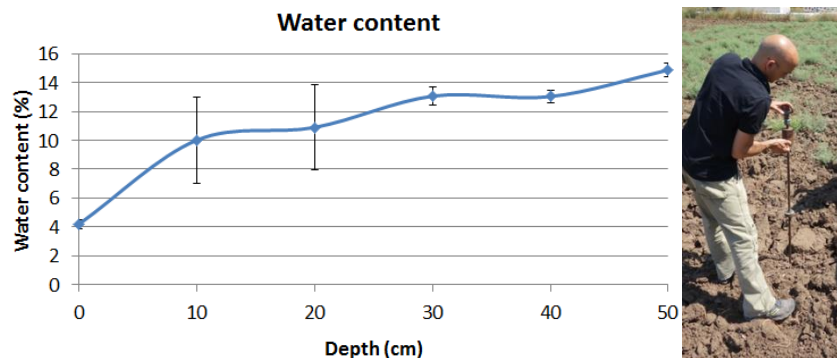


Fig.5: Soil water content results and the dynamic cone penetrometer test setup.

3 Numerical simulation

A numerical model was built using LS-DYNA dynamic FE code [7]. The tillage machine is represented by Lagrangian shell and solid elements. The agricultural clayey soil media is represented by 182,538 DE particles. Fig. 6 shows the soil tillage model with half blanked soil. The DE particles are separated to 5 parts in order to represent better the inhomogeneity of a plowed agricultural field. The coupling between the DE soil particles to the conveyor surfaces is defined by `*DE_TO-SURFACE_COUPLING`, surface velocities were defined by the variables: `LCVx` and `LCVz`. The rear conveyor vibrates vertically, causing the small soil particles to drop through its gaps while the large particles drop from the edge of the machine on top of the small particles. The model was solved by LS-DYNA code version SMP_s_Dev_113361 [7].

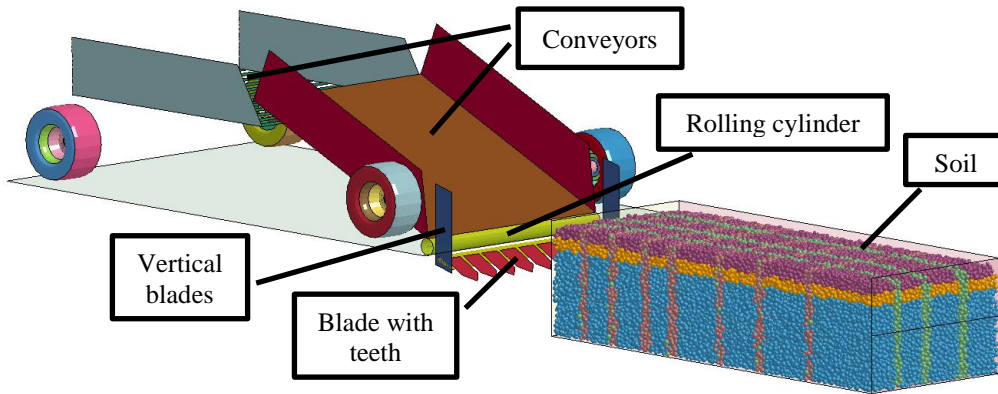


Fig.6: Soil tillage model (soil half blanked).

The DE soil parts are defined by `*MAT_ELASTIC` and `*DEFINE_DE_BY_PART` keywords. The particles radius is distributed in the range of 15 to 25 mm. The cohesion in the soil was modeled by capillary forces which are implemented in LS-DYNA according to Rabinovich et. al [8] as presented by Teng [9]. Equations 1-4 describe the capillary tension force in case of $0 < d_{int} < d_{crit}$ where d_{int} is the distance between two particles and d_{crit} is their critical rupture distance.

$$F_n = - \frac{2 \cdot \pi \cdot \text{Gamma} \cdot \bar{r} \cdot \cos(\text{CAPANG})}{1 + \frac{d_{int}}{d_{sp/sp}}} \quad (1)$$

$$\bar{r} = \frac{2 \cdot r_1 \cdot r_2}{r_1 + r_2} \quad (2)$$

$$d_{sp/sp} = -d_{int} + \sqrt{d_{int}^2 + 2 \frac{V_{LB}}{\pi \cdot \bar{r}}} \quad (3)$$

$$V_{LB} = \frac{4}{3} \pi (r_1^3 + r_2^3) \frac{1}{10} \text{CAPVOL} \quad (4)$$

Where Gamma is the liquid surface tension, r_1 and r_2 are the particles radiuses, CAPANG is the contact angle and V_{LB} is the liquid bridge volume as presented in Fig. 7 according to Teng [9].

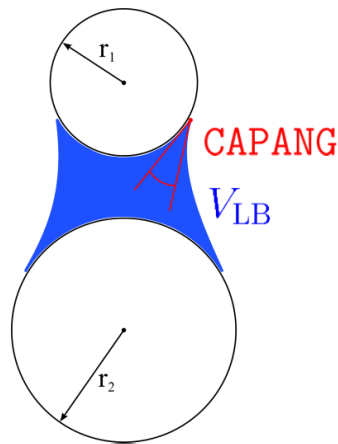


Fig.7: LS-DYNA capillary parameters according to Teng [9].

Two particles will be separated when the separation distance between them reaches the critical rapture distance in which the capillary force will drop to zero. The critical rapture distance According to Teng (2016) is calculated according to the following equation:

$$d_{crit} = \left(1 + \frac{CAPANG}{2}\right) \cdot \sqrt[3]{V_{LB}} \quad (5)$$

According to the equations presented above and normalization with respect to the particle's area, the capillary stress between two particles with 20 mm radius (the average radius used in the model) was calculated. Fig. 8 shows the absolute capillary tension stress as function of the distance between the two particles for different parts representing the soil media. The changed variable between the different parts is **GAMMA** that changes the capillary force magnitude. The contact stress, which acts in an opposite direction to the capillary stress, is plotted here by a red segmented line. The contact stiffness used in the model (Kn) is 1500 N/mm. The intersection points between the contact stress line and the different absolute capillary stress lines represent the stabilization points between two particles. Since usually the slope of the contact stress line is higher than the slopes of the capillary stress lines, the maximum capillary tension stress will act at zero distance between the two particles. The model's capillary variables were calibrated according to the field penetrometer test results which will be presented at the results chapter.

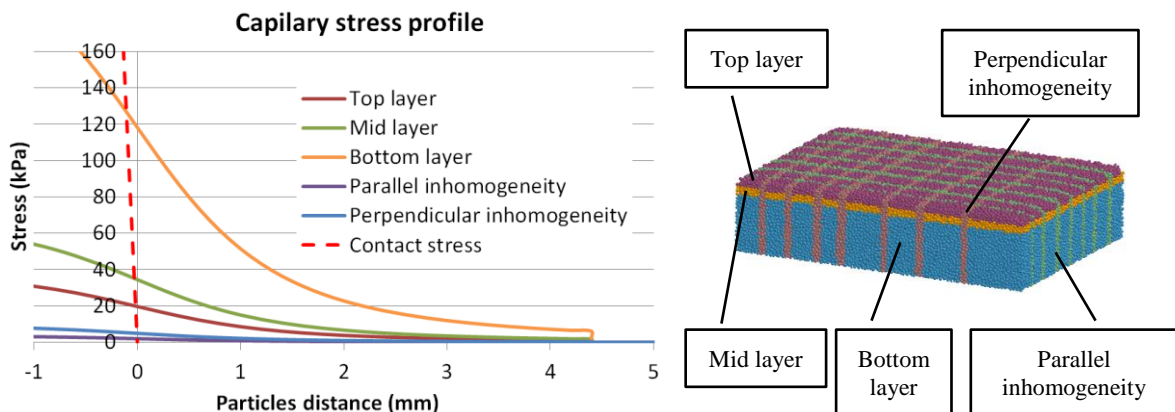


Fig.8: Average capillary particles tension stress as a function of their distance.

A model of the in situ dynamic cone penetrometer test was built in order to calibrate the DE particles variables. The penetrometer is represented by two parts: the cone penetrator and the drop weight as presented in Fig. 9. The soil used in the model is a section of the same soil particles used in the tillage machine model. The arbitrary blows of the drop weight were controlled using multiple two steps ***BOUNDARY_PRESCRIBED_MOTION_RIGID** (BPMR) keywords. Initially the model was left to stabilize under gravity. The first step of BPMR was activated after stabilization using **BIRTH** variable. In this first step the drop weight was lifted to 5 mm above the impact base of the cone penetrator. Afterwards the first BPMR command was removed by using **DEATH** variable. Then the second step of BPMR was activated using **BIRTH** variable. In this second step the drop weight was given an equivalent velocity downwards that represents a drop of 50 cm height as performed in the experiment. Afterwards the second BPMR command was removed by using **DEATH** variable. This procedure gave the drop weight a velocity towards the impact base of the cone penetrator. By creating more commands of these two steps with time intervals between them for allowing system stabilization, the weight drop procedure of the experiment was simulated.

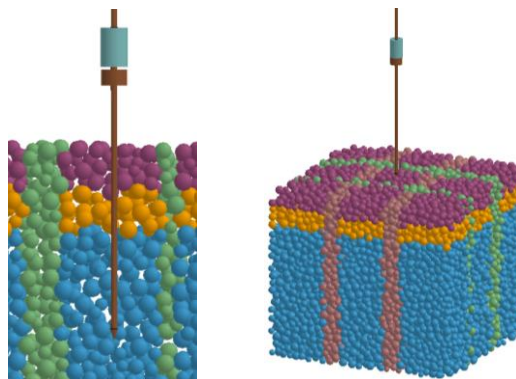


Fig.9: Dynamic cone penetrometer model.

4 Results

During the simulation of the dynamic penetrometer, the data of the cone penetrator and the drop weight were written to **ASCII** variable **RBDOUT**. Fig. 10 shows the displacement of the cone penetrator and the drop weight during the simulation and the vertical stresses developed during the penetration to the soil. Due to the elastic nature of the particles contact, at points of high particles densities some elastic rebounds may occur as can be noted in the plot at 2.5, 2.8 and 6.7 seconds where the drop weight jumped because of the particles elastic rebound. This behavior does not represent the correct plastic nature of the soil; however it should not interrupt the tillage process simulation in which no confined high velocity impacts occur.

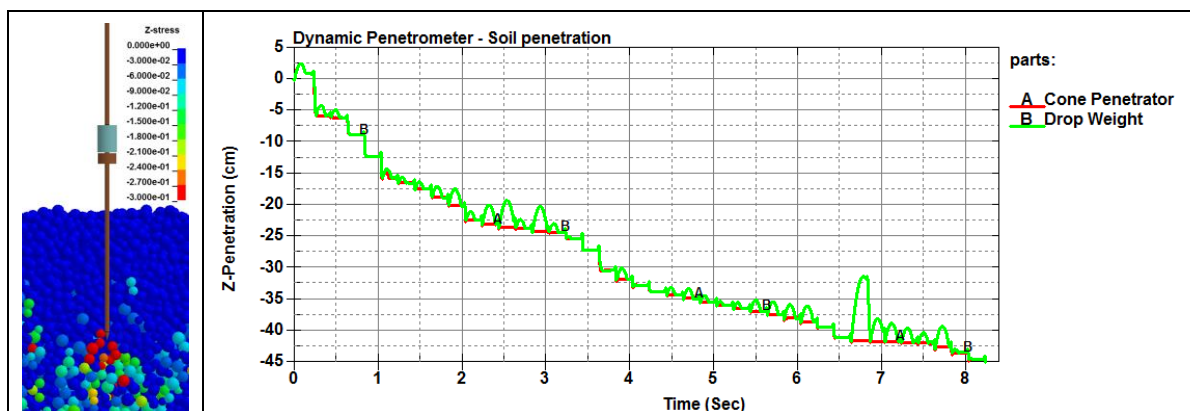


Fig.10: Dynamic cone penetrometer simulation results: vertical stresses and penetration plot.

The number of blows was counted from the simulation for segments of 5 cm penetration as performed in the field experiment. The capillary **GAMMA** variables of the DE soil parts were calibrated according to the results of the experiment. A comparison between four dynamic penetrometer simulation results to four field experiment results with standard deviation bars is presented in Fig. 11. The ordinate presents the number of weight blows required for 5 cm penetration of the cone penetrator into the soil. According to the results of the experiment, the soil stiffness increased to a depth of 30 cm and remained approximately constant to a depth of 45 cm. Considering the relatively large size of the particles in the simulation, there is a good agreement between the simulation and the experiment results. The calibrated soil parameters were used in the tillage machine simulation.

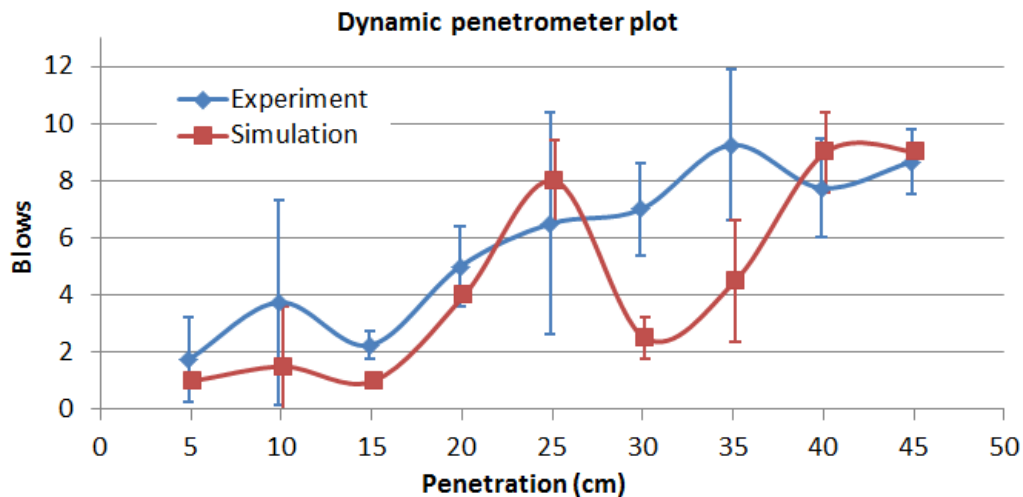


Fig. 11: Comparison of the number of dynamic cone penetrometer blows between the simulation and the field experiment.

A representative example of a soil tillage simulation scenario is presented in Fig. 12. During the simulation the front blade cuts through the soil and directs it onto the conveyor system. At the beginning of the simulation the soil and the tillage machine stabilize under gravity. The wheels are inflated with ***AIRBAG_SIMPLE_PRESSURE_VOLUME** keyword and are stabilized against a rigid surface. Since the front wheels have a significant component in the developed drag forces, as will be presented later, they move during the first stage of the simulation onto the DE particles of the soil to account for the bulldozing drag forces developed during the sinkage of the wheels.

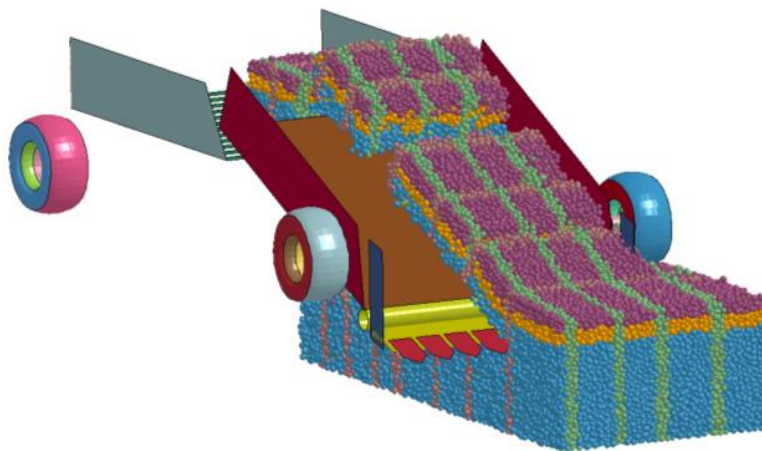


Fig. 12: Soil tillage simulation result.

During the field experiment two different front blades were examined. A long blade 52.5 cm long at 19° and a short blade 37.5 cm long at 27.5°. Fig 13. shows two FE models of the blades one on top of the other in a single figure in order to give a perspective on the differences of their size and orientation with respect to the rolling conveyor cylinder. The short blade is 1.5 cm lower than the long one.

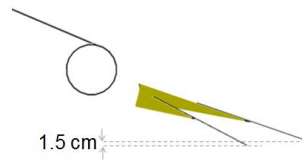


Fig.13: Orientation of the long and short blades.

The sum of the total drag forces required for the soil tillage at the simulation was compared to the sum of drag forces measured by the two force transducers at the experiment. Fig. 14 shows a comparison of the drag forces for the two blades. The results of the simulation predicted the results of the experiment with good accuracy. The forces obtained by the long and less inclined blade are about 30% lower from the forces obtained by the short and more inclined blade. The average drag force developed at the experiment with the long blade was about 4 Ton comparing to 6 Ton using the short blade. This significant increase in drag forces is directly related to expensive waste of energy.

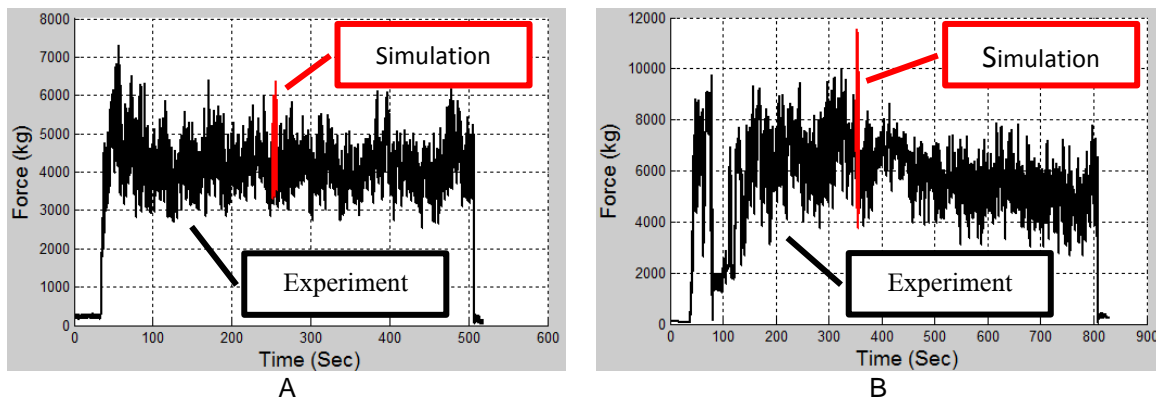


Fig.14: Drag force comparison: A. Long blade B. Short blade.

One of the useful benefits of a simulation comparing to an experiment is the ability to measure the force distribution on the components of the system without the need of complicated measuring system. Fig. 15 shows the drag forces developed on each component of the machine in the simulation filtered at 20 Hz. As expected, the largest force acts on the front conveyor blade which approximately ranges from 1 to 4 Ton. However according to the simulation results a significant drag force acts also on the front wheels which approximately ranges from 0.5 to 2 Ton. At initial stages of the research the tillage machine was modeled without its wheels but in that case no good physical agreement could be obtained with the results of the experiment. At a later stage the necessary wheels were added. The conveyor cylinder and the vertical blades each develop drag force of about 0.5 Ton. Further in this research an experiment setup will be designed in order to verify these results.

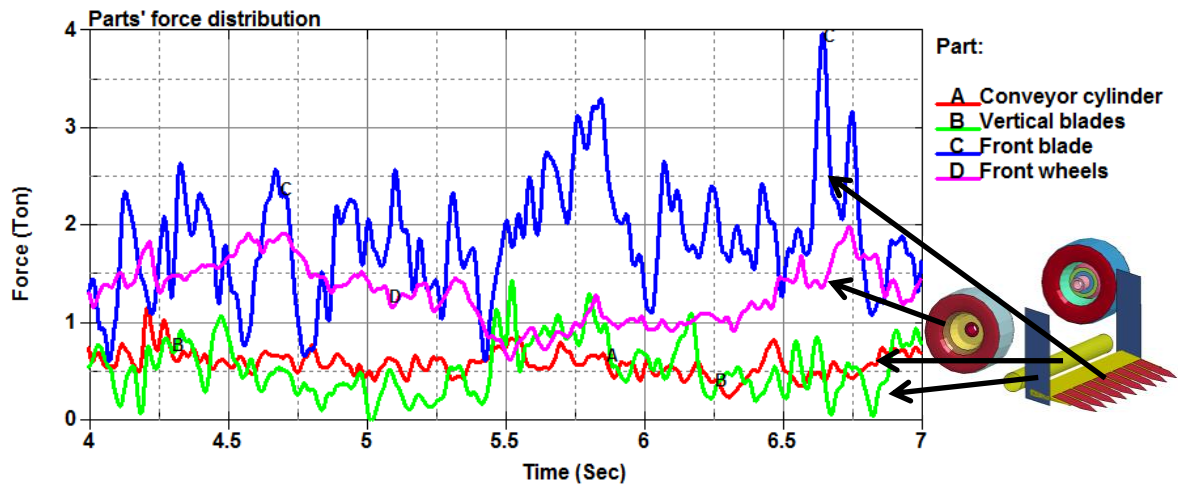


Fig.15: Drag force distribution on different machine parts.

Soil tillage is a process with high friction forces. As a result, during the operation of the tillage machine at field the blades are subjected to high wear. In order to improve the design of the machine for better wear durability, a qualitative examination using the DE wear prediction mode of LS-DYNA was performed. Several wear laws were implemented into LS-DYNA. In the current model the default Archard's wear law was used as presented by Teng [9]. The **WEAR**C variable was set to unity for the different parts of the machine. Fig. 16 shows the areas that are subjected to high wear as predicted by the simulation. The critical areas as predicted by the simulation are the front blade's teeth edges and at several areas on the vertical blades. The simulation also predicted some wear on the conveyor. Future work will focus on quantitative calibration and verification against experiments. The areas exposed to high wear will be considered in future machine design for improving wear durability at minimal cost.

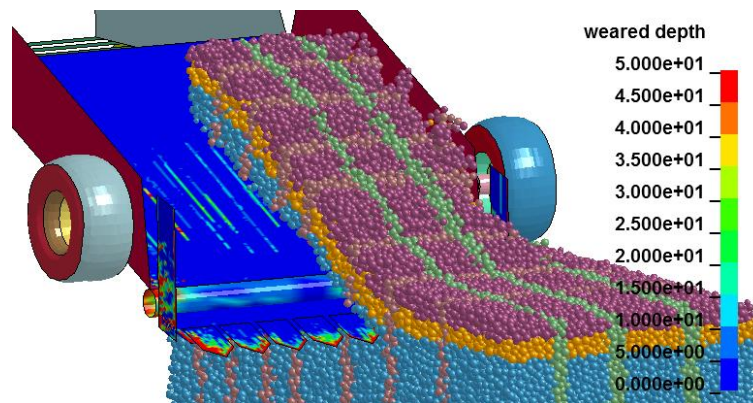


Fig.16: Relative wear on different machine parts.

The results show that LS-DAYNA DE simulations combined with experiments for calibration and validation are well suited for simulating soil tillage process. The simulation quantified the distribution of the forces on the different machine parts during the soil tillage which are difficult to measure at field experiment. The LS-DYNA DE wear tool can assist in future optimal machine design for wear durability. According to the results over 30% energy can be saved by different blade orientations.

5 Summary and conclusions

The reported work used LS-DYNA dynamic analysis for modeling a soil tillage machine by Lagrangian elements and plowed agricultural clayey soil by cohesive Discrete Element (DE). The simulation was calibrated and validated by full scale experiments using the soil tillage machine pulled by a tractor at an agricultural field. During the experiments two types of blades were compared at different tillage depths. Using the advantages of the simulation, a drag force distribution over the different parts of the machine was obtained. The research demonstrated that LS-DYNA DE simulations are well suited for simulating soil tillage process in which also a prediction of the expected wear is provided.

The results of the research show that over 30% power reduction can be obtained by optimal design of the blade shape, angle and position relative to the pickup conveyor using LS-DYNA DE model simulation.

Future work will focus on several aspects:

1. Development of a system for measuring vertical and drag forces acting on the wheels of the tillage machine at experiments for improving model validation.
2. Examination by simulations and experiments the developed drag forces with different heights of the blade relative to the rolling cylinder of the conveyor
3. Examination of different blade designs by simulation for better energy efficiency and wear durability of the machine.
4. Examination of the tillage process at several depths by the simulation tool and field experiments for improving the calibration of the model parameters.

6 References

- [1] Asaf Z., Rubinstein D., Shmulevich I. "Comparison of the shear stress–displacement relationships of semi-empirical and discrete-element models ", Ninth European ISTVS Conference, 2003.
- [2] Asaf Z., Rubinstein D., Shmulevich I. "Evaluation of link-track performances using DEM ", J. Terramechanics, 2006, 43(2):141-161.
- [3] Asaf Z., Rubinstein D., Shmulevich I. "Determination of discrete element model parameters required for soil tillage ", Soil & Tillage Research, 2007, 92(1): 227-242.
- [4] Shmulevich I., Asaf Z., Rubinstein D. "Interaction between soil and a wide cutting blade using the discrete element method", Soil & Tillage Research, 2007, 97(1): 37-50.
- [5] Shmulevich I., "State of the art modeling of soil – tillage interaction using discrete element method", Soil & Tillage Research, 2010, Vol. 111 No. 1, pp. 41-53.
- [6] Shmulevich I., Asaf Z., Catav R., "Discrete element modeling of cohesive grain materials", International Conference of Agricultural Engineering - CIGR-AgEng, 2012, pp.C-1499 ref.7.
- [7] LSTC, "LS-DYNA KEYWORD USER'S MANUAL", ed. 03/23/2015.
- [8] Rabinovich Y. I, Esayanur M. S., Moudgil B. M., " Capillary Forces between Two Spheres with a Fixed Volume Bridge: Theory and Experiment ", Langmuir, 2005, 21, 10992-10997.
- [9] Teng H., "Discrete Element Method in LS-DYNA ", LSTC, 2016.